A Bio-inspired Platform to Modulate Myogenic Differentiation of Human Mesenchymal Stem Cells Through Focal Adhesion Regulation

*Haiyang Yu, Chor Yong Tay, Mintu Pal, Wen Shing Leong, Huaqiong Li, Hai Li, Feng Wen, David Tai Leong, and Lay Poh Tan**

The use of human mesenchymal stem cells (hMSCs) in cardiac-tissue engineering has gained widespread attention and many reports have shown that matrix compliance, micro/nano-patterns could be some of the important biophysical cues that drive hMSCs differentiation. Regardless of the type of biophysical induction cues, cells mainly explore their environment via focal adhesion (FA) and FA plays an important role in many cellular behaviours. Therefore, it is hypothesized that FA modulation through materials manipulation could be an important cue for modulation that would result in the stem cell lineage commitment. In this work, the FA of hMSCs is modulated by a novel microcontact printing method using polyvinyl alcohol as a trans-print media which can successfully print proteins on soft polydimethylsiloxane (PDMS). The FA is successfully modified into dense FA and elongated FA by micropatterning square and rectangular patterns on 12.6 kPa PDMS respectively. Additionally, the combined effects of stiffness of PDMS substrates (hard (308 kPa), intermediate (12.6 kPa)) and FA patterning on hMSCs differentiation are studied. The results indicate that dense FA does not induce myogenesis while elongated FA can promote cytoskeleton alignment and further myogenesis on PDMS with intermediate stiffness of 12.6 kPa. However, on stiff substrate (308 kPa), with or without patterns, the cytoskeleton alignment and myogenesis are not obvious. This demonstrates for the first time that it is possible to induce the differentiation of hMSCs by regulating the FA using a materials platform even in the absence of any biochemical factors. It also shows that there is a synergistic effect between FA regulation and matrix stiffness that results in a more specific and higher up-regulated myogenesis. This platform presents a new chemical/biological-free method to engineer the myogenic differentiation of hMSCs.

1. Introduction

Millions of people are suffering from many soft organ diseases like heart attack and skin cancer every year resulting in a rapid development of soft tissue engineering.[1] In the USA alone, more than 1.5 million of people are suffering from myocardial infarction every year and research in heart tissue engineering is in high demand.[2] Human mesenchymal stem cells (hMSCs) continue to attract prominence due to their multipotent property and potentials in regenerative medicine, especially in heart tissue engineering.[3] Many studies have been shown that stem cells are sensitive to their microenvironment, and cell behaviors can be determined by the stem cells niches.[4] Amongst several induction factors, biophysical forces regulate important cellular processes, such as communication,[5] migration,[6] cell attachment and spreading,[7] and driving stem cell lineage commitment.[8] It was shown that soft, intermediately stiff and rigid substrates that respectively mimics brain, muscle and bone stiffness were able to drive the corresponding tissue specific differentiation.[9] Despite these promising findings, the actual mechanism of how matrix elasticity can drive hMSCs differentiation is elusive. The main hurdle faced in elucidating this fundamental mechanism is the current inability to experimentally segregate formation of focal adhesions (FAs) morphologies and density

H. Yu, Dr. C. Y. Tay, Dr. M. Pal, Dr. W. S. Leong, H. Li, Dr. H. Li, Dr. F. Wen, Prof. L. P. Tan
Division of Materials Technology
School of Materials Science and Engineering
Nanyang Technological University
50 Nanyang Avenue, 639798, Singapore
E-mail: lptan@ntu.edu.sg
H. Yu
Research and Development Unit
National Heart Centre Singapore
17, Third Hospital Avenue, Mistri Wing, 168752, Singapore
Prof. D. T. Leong
Department of Chemical and Biomolecular Engineering
National University of Singapore
4 Engineering Drive, 117576, Singapore

DOI: 10.1002/adhm.201200142

from their multi-modal responses to substrate stiffness and cellular morphology. FAs appear to be the connective node in this puzzle. Adherent stem cells sense the underlying substrate environment mainly via FAs; and then translate the "biophysical signals" into cellular responses through the cytoskeleton. This can then result in modulating cell lineage specific gene and protein expression inside the cell.[10] Most of the cell-materials interaction studies used homogeneously coated substrates[9a] or micropatterned (20–500 μm) surface[11] or nanopatterned substrate,[12] but few studies explored sub-cellular adhesions using micropatterning of single FA. Lehnert et al. made a study on the geometrical limits of ECM binding sites which is required for FA development for cell spreading using microcontact printing (μCP).[13] In another study, Xia et al. found that μCP of different shapes and sizes of ECM islets would affect FA development and then have an influence on cell motility and induce cell orientation and elongation via modulating of FA.[14] With the increasing importance of FAs in cell-materials interactions, we realized that it was pivotal to explore the role of FAs in stem cell differentiation to gain insights into cell materials interactions. But the use of FA modulation to induce stem cells differentiation is quite limited to date.

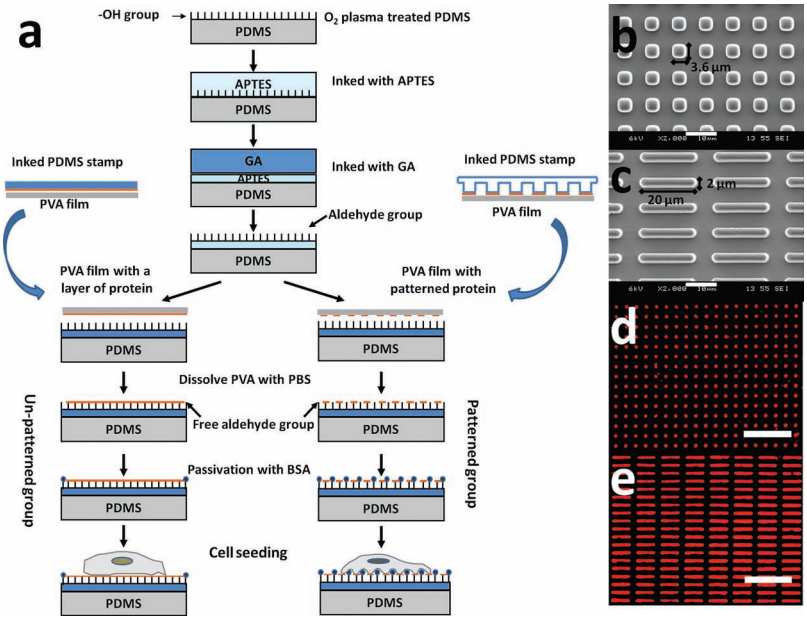

Figure 1. Novel microcontact printing (μCP) could effectively pattern COLI on soft and high stamp-adhesive PDMS substrates. (a): Schematic diagram of novel μCP procedure which uses a PVA film as a trans-print media instead of directly printing on the substrate. (b, c): SEM validation of stamp features of S3.6 (b) and L20 (c) patterns, respectively. The height of the features on the stamps was 5 μm. (d, e) Fluorescent images of Cy3-labeled patterned COLI showing novel μCP method could successfully print protein on 2.1 kPa soft and high stamp-adhesive substrates. Scale bar in (b) and (c) shows 10 μm, in (d) and (e) shows 50 μm.

Goffin et al. made a study of how elongated FAs affect myofibroblast maturation but they did not explore further to see the combined effects of FA patterning and matrix stiffness.[15] We reported earlier on the use of μCP to modulate the shape of hMSCs and found that elongated hMSCs with aligned cytoskeleton increased myogenesis. Moreover, the FA development between elongated hMSCs and normal spread hMSCs were found to be different.[9b] Implicit in these latter studies is the centrality of the FAs in regulating basic cellular behavior. With this, we set out to investigate the possibilities of modulating FAs specifically to drive stem cell differentiation.

We combined matrix compliance and extracellular enforced adhesion nodes through a novel μCP technique on polydimethoxysilane (PDMS) substrates of different compliance to coax the cells to adopt certain cellular shape or FAs configuration. We hypothesized that the matrix stiffness, combined with FA development (such as FA morphology and density) and cytoskeleton arrangement would affect hMSCs differentiation. This study has provided insights on the role of FAs and matrix stiffness in cell-materials interactions during hMSCs myogenic differentiation for possible future clinical muscle tissue engineering applications. Moreover, the novel μCP method expands cell-materials interaction study to soft and tacky surfaces in a simple and cost-effective manner.

2. Results and Discussion

2.1. PDMS Substrates of Various Stiffness and Two Different Micropatterns Were Evenly Printed on Substrates

The average shear storage moduli G' of 1:10, 1:50, and 1:70 PDMS were 102.7 ± 6.9 kPa, 4.2 ± 0.1 kPa, and 0.7 ± 0.1 kPa respectively. For rubber elastic materials, assuming a Poisson ratio of 0.5,[16] the Young's modulus E of 1:10, 1:50, and 1:70 PDMS was about 308 kPa, 12.6 kPa, and 2.1 kPa respectively. PDMS was chosen as the matrix since it has several properties that make it attractive as a common used material for micropatterning and topography modification. The ease of fabrication, non-toxicity, and easy tunable mechanical properties were critical in cell-materials interaction study.[17] The reason to choose the PDMS substrates with stiffness of 12.6 kPa and 2.1 kPa was that they mimicked muscle and brain environment respectively[18] with the 308 kPa group as a non-compliant control group on the other end of the spectrum. The control group we used was 308 kPa hard PDMS, the same material as 12.6 kPa and 2.1 kPa substrates, to eliminate the materials chemistry effects. This stiffness is reminiscent of bone which is biologically very different from muscle and thus the differentiation drivers are different.[19] μCP is a widely used technique to study cell behaviours[20] but conventional μCP is not easy to be performed on soft and/or tacky substrates, such as polydimethylsiloxane (PDMS) with a Young's modulus lower than 12.6 kPa.[21] Therefore, a simple and novel micropatterning technique was developed using polyvinyl alcohol (PVA) as a trans-print media which can efficiently be used on soft and/or tacky substrates.[22]

SEM images (**Figure 1**b-c) for the surface topographies fabricated on PDMS stamps and immunostaining images (Figure 1d-e) of the printed COLI on PDMS substrate were validated as shown in Figure 1. Pattern in Figure 1b named S3.6 was a square with dimension of 3.6 × 3.6 μm, which was designed to induce dense FAs development. The pattern in Figure 1c named L20 consisted of rectangular islets, with the size of 20 × 2 μm, was designed

to induce elongated FA according to previous report.[15] The distance between islets of both of the two patterns was 6 μm. This was the optimal distance that allows cells to develop FAs across the islets.[13,23] If the distance is too large, cell may not be able to cross the islets and cell spreading will be restricted. If the distance is too small, cells may not be able to distinguish between the islets. Although the optimal distance may depend on matrix stiffness, we want to decouple the patterning effect from stiffness effect by having a constant islet spacing across all matrix stiffness. Transfer printed patterns of COLI on PDMS substrates were labeled with Cy3 (red) as shown in Figure 1d-e which indicated that the novel trans-print μCP method could efficiently transfer the protein patterns onto soft and tacky PDMS substrates.

2.2. Micropatterning Has Most Significant Influence on FA Development for Intermediate Substrates

A screening gene transcription study of the effects of matrix stiffness (308 kPa, 12.6 kPa and 2.1 kPa PDMS substrates) was performed using un-patterned group on hMSCs differentiation by qPCR. As shown in Figure S1b, there was an indication that hMSCs were induced into myogenic lineage commitment (albeit not entirely specific) by PDMS substrates with a stiffness of 12.6 kPa, which mimicked the muscle micro-environment stiffness.[9a] On the other hand, neurogenic lineage commitment was shown by cells on PDMS with a stiffness of 2.1 kPa, which was comparable to brain environment[9a] (in Supporting Information (SI)). Conversely, the hMSCs on 308 kPa PDMS did not show any myogenesis or neurogenesis (data not shown). Therefore, 12.6 kPa PDMS which could promote myogenesis of hMSCs was selected in the following studies based on our interest in heart tissue engineering, with the 308 kPa as the control group.

From Figure S2, we can see that the FA density and cytoskeleton development decreased on softer substrates. Since the stress fibers of a cell connect to its niche via FAs, it is reasonable to believe that the extracellular FA patterning would affect the development of FAs and as a consequence, the stress fibers would re-organize into a feedback loop.[24] Here, microcontact printing of sub-cell size islets was used to manipulate FA development. Prior to that, a passivation study was needed to validate the blocking agent performance. The study was performed with a 20 μm width strip pattern to show 2% BSA was able to passivate the non-patterned region well for at least 9 days (indicated by the fact that cells only grew within the strip pattern in Figure S3). The passivation study verified the patterning efficiency of the platform.

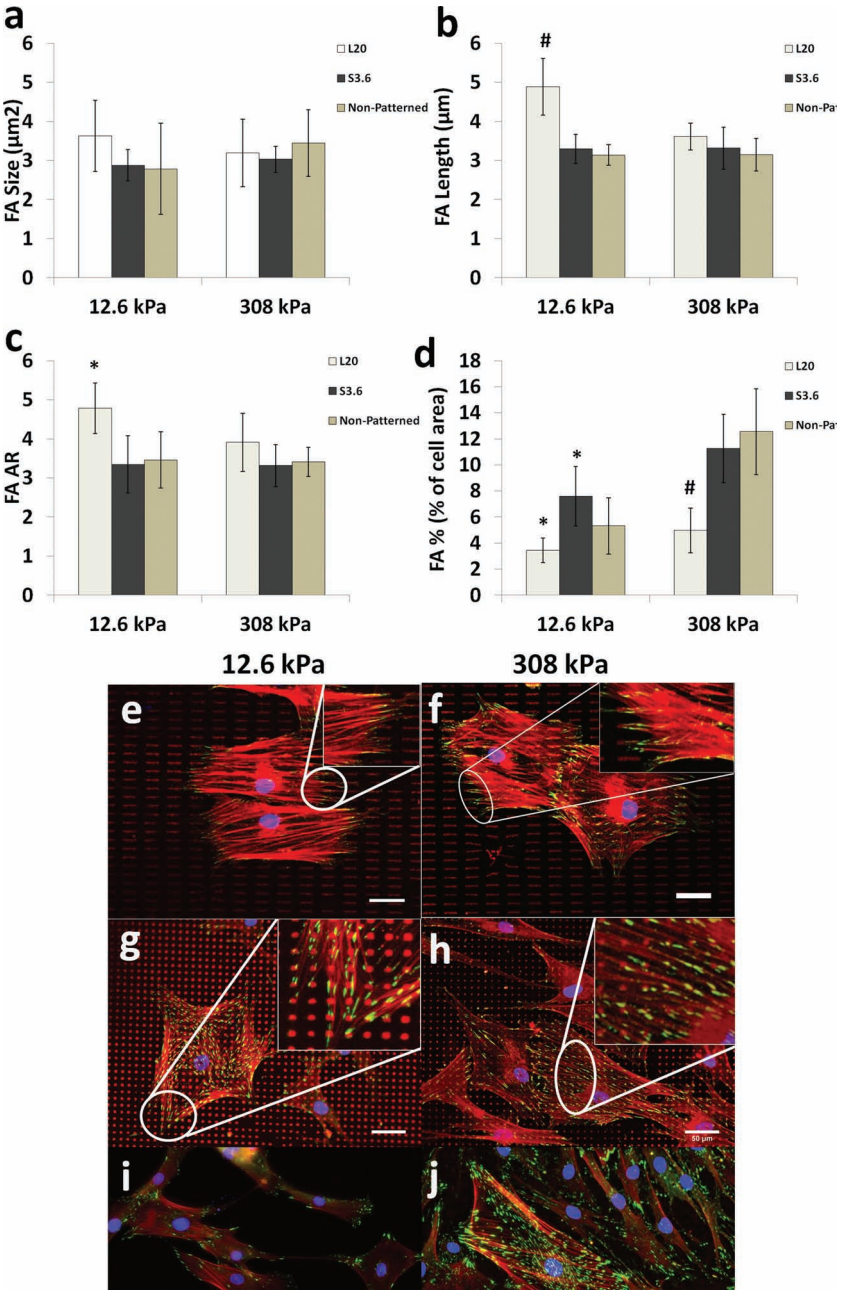

Figure 2. Micropatterns affect FA development on 12.6 kPa PDMS substrate on day 7. (a–c): statistical studies of FA morphology showing that L20 and S3.6 have no effects on FA size while L20 could significantly induce elongated FA only on 12.6 kPa substrate. (d): S3.6 could increase FA density on 12.6 kPa substrates. Bars represent mean ± standard deviation. $*p < 0.05$ and $\#p < 0.01$ compared with non-patterned groups (n = 3). (e–j): Fluorescent images showing different vinculin (green) and F-actin (red) development in cells on PDMS with L20 pattern (e,f), S3.6 pattern (g,h), and without patterns (i,j), respectively. COLI patterns were labeled with Cy3 (red) in (e–h) and the nucleus was labeled with DAPI (blue). Scale bars shows 50 μm.

Figure 2 shows the FA development of the cells when cultured on the two substrates of 12.6 and 308 kPa with different patterns. On intermediate stiffness (12.6k Pa, Figure 2a), the FA

size was not significantly affected by different patterns. However, the FA length and FA aspect ratio (AR) were significantly higher in the L20 pattern as compared to S3.6 and the control; indicating the elongation of the FA in the former group. Whereas, high FA density was induced in the S3.6 pattern while in L20 the density was significantly lower. This result is amazing since the L20 rectangular pattern is actually denser than the S3.6 square pattern. It indicated that cells would develop FA not only based on the density of the pattern, but more so in accordance to the shape of the pattern. It is remarkable to observe the dominant effect of patterning morphology on FA development. The statistical result in Figure 2 showed that the aim to induce elongated and dense FA was achieved by L20 and S3.6 patterns respectively.

On the hard substrate (308 kPa), the outcome was completely different where there was no apparent trend in the FA size, FA length and FA AR when cultured on different patterns. Both the S3.6 and L20 patterns did not induce significant changes in the FA development; with the exception of FA density; and remained similar to the control. Interestingly, for FA density, just like on intermediate stiffness substrate, L20 pattern induced significantly lesser density as compared to both S3.6 and control. This study seems to show that patterning had less impact on FA development when a stiff substrate was used.

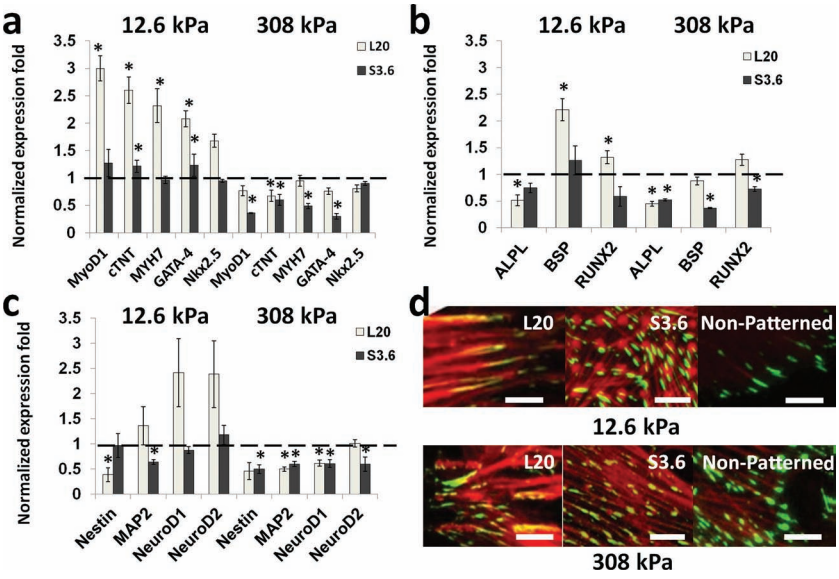

Figure 3. The interplay of FA development and matrix stiffness on hMSCs differentiation at transcription level on day 7. L20 could induce myogenesis as shown in (a, left) while showed less effect on osteogenic markersand neurogenic markers (b and c, left). But the FA modulation effects were not obvious on 308 kPa substrates (a, b, c, right). Relative gene expression levels were normalized to non-patterned group as indicated by the dashed line. Bars represent mean ± standard deviation. The asterisks indicate statistic significant difference ($p < 0.05$) compared with non-patterned groups. The small panels in (d) were vinculin (green) and F-actin (red) staining indicating how patterns affect FA development. Scale bar in (d) shows 10 µm.

The reason could be due to the fact that cells would develop a larger and more stable FA when cultured on a stiff substrate,[25] and the effect of this matrix stiffness was so dominant that it dictated the behavior of FA development. In this case, the effect of patterns was overshadowed and could not be manifested (Figure 2f,h), reflected by the fact that FAs were not as elongated and cytoskeleton was not as well aligned as on 12.6 kPa PDMS. However, on the 12.6 kPa substrate, the effect of stiffness was significantly reduced and this allowed L20 pattern to control the FA development resulting in aligned cytoskeleton and elongated FA as shown in Figure 2e. L20 pattern could significantly increase the FA length by 48% and FA AR by 38% as compared to un-patterned group (Figure 2b-c) when cultured on 12.6 kPa substrate. This was accompanied by a slight decrease in FA density, same as what we observed in our previous study[9b] (Figure 2d). On the substrate of the same stiffness, S3.6 increased FA density without altering the morphology (as compared to control) and this resulted in random orientated cytoskeleton (Figure 2g). This is an important indication that on tissue compliant substrates, the FA of hMSCs could be manipulated via this micropatterning platform. With this, we moved on to relate FA development to stem cell differentiation.

2.3. Effects of FA Modulation via Micropatterning on hMSCs Differentiation

By assaying for transcript levels of lineage-commitment genes with qPCR, we looked specifically at whether changing the FA size and length through the two micropatterns helped hMSCs differentiation at biomolecular level. Using proximity ligation assay (PLA) targeting myosin heavy chain (MHC) and conventional immunostaining confirmed the observation at protein level. Relative gene expression at 7th day for cells cultured on intermediate and stiff substrates with both patterns was shown in **Figure 3**a-c and Figure 3d showed the fluorescent images of FA development.

On 12.6 kPa PDMS, S3.6 pattern did not elicit obvious effect on the differentiation of cells. However, the trend was completely different when cells were cultured on the same substrate (12.6 kPa) but with L20 pattern. Up regulation of myogenic markers: MyoD1, GATA-4, MYH7, and cTNT, by 2–3 times was evident whereas no significant effect on neurogenic and osteogenic lineage commitment was observed. To further confirm that the up-regulated myogenic genes were functionalized at protein level, we employed PLA to quantify the expression of MHC (coded by MYH7). From **Figure 4**a and 4b, there was an apparent increase in the MHC expression (red dots indicted by arrow) for the cells cultured on L20 pattern of 12.6 kPa substrate stiffness as compared to the control. When the expression was quantified using PLA dots density, it showed a dramatic increase by nearly 76% (Figure 4c) as compared to hMSCs on non-patterned 12.6 kPa PDMS. Conventional fluorescent immunostaining of MHC (Figure 4d), MAP2 (neurogenic marker, Figure 4e), RunX2 and Ocal (osteogenic markers, Figure 4f-g) was also performed, but only MHC showed significant increased expression, indicating specific myogenesis.

On 308 kPa PDMS substrate, cells did not significantly change their genes expression of the three lineage markers studied. But all genes were down regulated in both S3.6 group

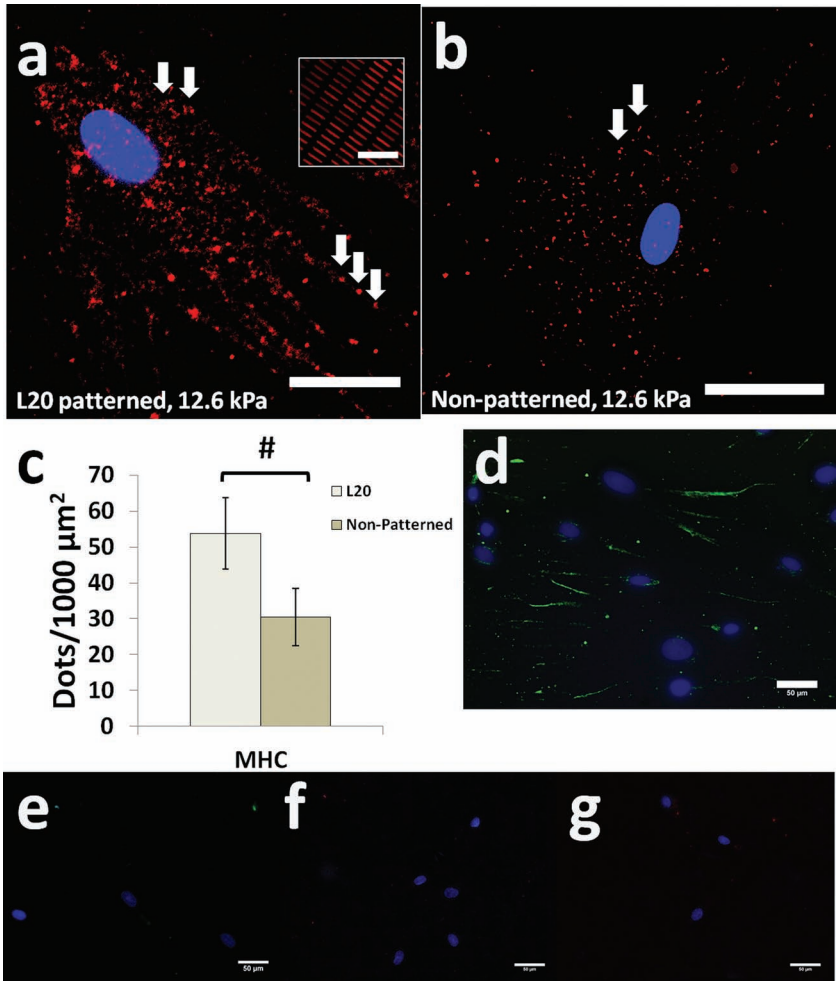

Figure 4. L20 significantly increased MHC expression on 12.6 kPa substrate verified by PLA. MHC (red, typical dots indicated by white arrow) of cells on L20 patterned (indicated by the small panel at the upper right) 12.6 kPa PDMS (a) showed a higher expression than that of cells on non-patterned (b) 12.6 kPa PDMS. (c): Statistical study of MHC density. $\#p < 0.01$ (n = 26). (d–f) showed conventional immunostaining images of MHC (d), MAP2 (e), RUNX2 (f), and Ocal (g). Scale bar shows 50 µm.

and L20 group. These results clearly showed that there was an interaction between the matrix stiffness and FA patterning in affecting differentiation. If these physical conditions were optimally formulated, the differentiation towards a certain lineage could be induced as shown in our studies for myogenesis (elongated FA and 12.6 kPa stiffness). However, if one of the physical cues was too dominant (very stiff substrate in our case), it would suppress the effects of other physical cues (patterning in our case).

From these results, we postulated that elongated FA and consequently aligned cytoskeleton were strongly correlated to the stem cell lineage commitment. On 12.6 kPa L20 patterned PDMS, cells showed elongated FA as indicated by statistical studies in Figures 2b and c, and immunostaining pictures in Figure 2e. Since FA was linked to actin filament, elongated FA of cells on L20 patterned PDMS with intermediate stiffness of 12.6 kPa induced aligned cytoskeleton compared to non-patterned group as shown in Fast Fourier Transform (FFT) images in **Figures 5**b and 5d (generated by ImageJ). Previous reports have shown that elongated "supermature" FAs (suFAs) were found during human myofibroblast differentiation.[26] These suFAs regulated stress fiber formation and cellular tension.[27] In our study, we found that this kind of elongated FAs would recruit integrin β_3 (ITB3) to form larger and elongated clusters and increase the expression of myosin light chain kinase (MLCK), which is a contraction indicator in cells, compared to un-patterned group (Figure 5e). Therefore, both elongated FA and aligned cytoskeleton were postulated to contribute to up-regulation of myogenic markers as depicted in the model presented in Figure 5f. In the model, elongated FAs could transmit the mechanical signals into the cell nucleus,[28] which in turn activate cell response such as recruitment of integrin cluster formation, alignment of stress fiber in a particular direction, and also recruiting MLCK to exert the appropriate cellular tension for myogenesis.[15] MLCK is actively involved in cellular contraction regulation. It cooperates with myosin-IIA, which would then associate with the actin filament to create contraction along the cytoskeleton and promote stress fiber assembly, and further affect cell lineage commitment.[29] Higher expression of MLCK in cells with elongated FA (Figure 5e) indicated higher contraction inside the cell as compared to that of the un-patterned group. The actin cytoskeleton which was closely associated with cellular tension might also play a part.[30] In native myotubes, cytoskeleton is found to be well organised and aligned which is logical as it helps in the function of anisotropic contractility and tension.[31] However, the tension should be in optimal range which may trigger some signalling pathway necessary for myogenesis and matrix stiffness which will affect the cytoskeleton tension and FA development should be within myogenic environment as well. The potential signalling pathway involved in this study is currently being pursued.

3. Conclusions

In summary, our results showed that elongated FA and aligned cytoskeleton is essential for cell commitment towards myogenesis. By optimally combining FA patterning (to induce elongated FA) with matrix stiffness, we have shown for the first time that there is a synergistic effect on specific myogenic differentiation. This up-regulation involved elongated FAs which would recruit integrin β_3 and MLCK, thereby increasing the cellular tensions and promoting myosin heavy chain synthesis. It is necessary to note that this specific lineage commitment

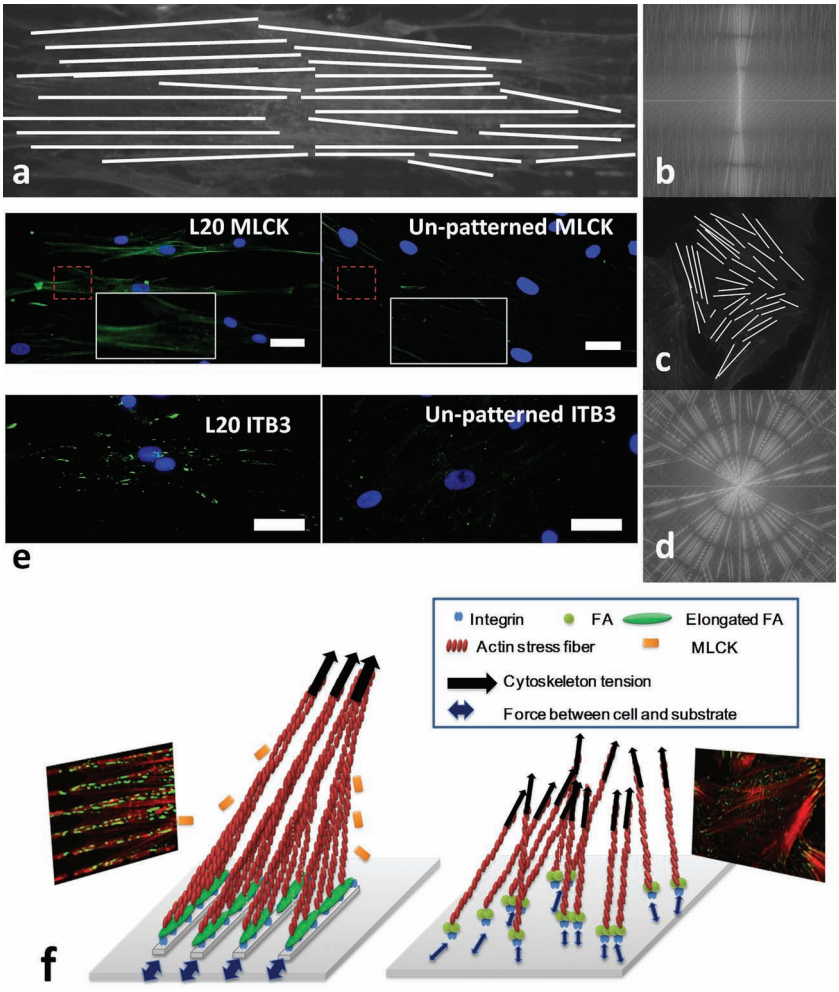

Figure 5. Elongated FA and proper cellular tension give myogenesis. (a) F-actin of L20 patterned hMSC on 12.6 kPa PDMS was manually marked. (b) FFT of L20 showed specific alignment of cytoskeleton. (c) F-actin of non-patterned hMSCs on 12.6 kPa PDMS show disorganized arrangement. (d) FFT of (c) showed random distribution of cytoskeleton. (e) Showed that hMSCs on L20 patterned 12.6 kPa PDMS exhibited higher expression of MLCK and integrin $\beta 3$ (ITB3) compared with cells on 12.6 kPa un-patterned PDMS. Scale bar shows 50 µm. (f) Schematic chart showed the interplay between FA modulation, cellular tension, matrix stiffness, and cytoskeleton arrangement.

took place in the absence of any induction medium, but purely driven by manipulation of cell–materials interaction. This work will prove to be a useful tool to induce stem cell differentiation in the future, especially in the field of cardiac tissue engineering where scaffolds could have two-fold functions of support and acting as a platform to modulate stem cell differentiation.

4. Experimental Section

Cell Culture: Cryopreserved hMSCs (Cambrex), derived from human bone marrow, were cultured as previously described.[32] During the experiments, cells were cultured in DMEM low glucose medium (Sigma) supplemented with 10% FBS (PAA) and 1% penicillin/streptomycin (Nagase) at 37 °C, 5% CO_2. The experiments described herein were performed using cells from passage 5.

Substrate Fabrication and Characterization: To prepare substrates of different stiffness, PDMS (Sylgard 184, Dow Corning) with three types of cross link ratio (1:10, 1:50 and 1:70 kPa, cross linker: base) were used. The pre-polymer solution was poured into 35 mm culture dish (1.5 mL each), and the dishes were baked in vacuum oven for 30 min to remove air bubbles. Afterwards, the pre-polymer was cured in an oven at 65 °C for 24 h. PDMS shear elastic modulus was measured using a Rheometer (Physica MCR 501, Anton Paar) according to the instruction provided by the manufacturer.

Fabrication of Elastomeric Stamp and Inking: The silicon master templates bearing the desired topographic features were fabricated by standard photolithography and were pretreated with 1% octadecyltrichlorosilane (OTS) (Sigma). 1:10 (cross linker: base) liquid PDMS was cured against the master at 100 °C for 3 h then the PDMS layer was gently peeled off as the stamp with a dimension of 1.5 cm × 1.5 cm. For no-feature stamp fabrication, mold casted 1:10 PDMS was cut into round shape with a diameter of 22 mm as the stamp without patterns. The fabricated elastomeric stamps were sputtered coated (SPI-MODULE coater) for 40 s, and then were examined under a scanning electron microscopy (SEM) (JEOL 6360).

For inking, the PDMS stamps with or without pattern features were immersed with 200 µg/ml collagen type I (COLI) (rat tail, Invitrogen) in acetic acid (50 mM, Sigma) in deionized water for 1 h, followed by blow drying with pressurized purified nitrogen gas.

Micropatterning of hMSC: The µCP was modified from the method described by Li et al.[33] and the procedure was illustrated in Figure 1a. Briefly, the PDMS substrates were treated with oxygen plasma in a plasma cleaner (PDC-002, HARRICK) with a power of 10.8 W for 1 min at a pressure of 120 mTorr followed by inking with 2% (3-aminopropyl) triethoxysilane (APTES) (Sigma) in 90% ethanol for 40 min. After that, substrates were washed with 100% ethanol and dried in a 60 °C oven for 1 h then immersed in 2.5 wt% glutaraldehyde (GA) (Sigma) in phosphate buffered saline (PBS) for 1 h followed by washing with Milli-Q water for 1 h.

To prepare PVA film, 0.5 wt% of PVA (Sigma) in deionized (DI) water was prepared and left at room temperature overnight, followed by magnetic stirring at 90 °C for 2–3 h in a bottle with cap to dissolve the PVA particles completely. PVA solution (20 mL) was poured into a glass petri dish (150 × 20 mm). The PVA solution was air dried in a laminar flow hood for 18 h to form the film. The dried PVA film was removed from petri dish and was cut into round film by a SCHMIDT® Presses (SCHMIDT Technology, Germany) to be used as the trans-print media. The thickness of the film h was determined as:

$$h = \frac{m}{\rho A} \quad (1)$$

where m was the mass of PVA used, ρ was the density of PVA (1.29g mL^{-1} according to manufacturer's data), and A was the area of the Petri-dish. The thickness of the PVA film was about 44 µm in our study.

Inked stamp with a layer of COLI (named non-patterned group) or patterned COLI was placed in conformal contact with PVA film in a laminar flow hood for 30 min instead of directly printing on the target substrate. The patterned side of the film was placed onto the PDMS substrate and was left for 30 min. After that, PBS was applied to rinse the

Table 1. Primer sequence and product size for qRT-PCR.

Genebank accession number	Gene target	Primer Sequence (5′-3′)	Product size (bp)
NM_001101	β-actin	Sense: CATGTACGTTGCTATCCAGGC	250
		Antisense: CTCCTTAATGTCACGCACGAT	
NM_002046	GAPDH	Sense: CATGAGAAGTATGACAACAGCCT	113
		Antisense: AGTCCTTCCACGATACCAAAGT	
BC021289	Alkaline phosphatase (ALPL)	Sense: CTCTCCAAGACGTACAACACC	201
		Antisense: AATGCCCACAGATTTCCCAGC	
NM_004967	BSP	Sense: TGGATGAAAACGAACAAGGCA	200
		Antisense: AAACCCACCATTTGGAGAGGT	
NM_004348	Runt related transcription factor 2 (RUNX2)	Sense: TCCTATGACCAGTCTTACCCCT	190
		Antisense: GGCTCTTCTTACTGAGAGTGGAA	
NM_002478.4	Myoblast differentiation protein 1 (MyoD1)[39]	Sense: CGGCGGCGGAACTGCTACGAA	459
		Antisense: GGGGCGGGGGCGGAAACT	
NM_153813	GATA-4	Sense: GACAAGGGCGTCCAGACTC	140
		Antisense: TGCGAGGAGCAGTAATACTTCTT	
NM_000257	MYH7	Sense: CACTGATAACGCTTTTGATGTGC	165
		Antisense: TAGGCAGACTTGTCAGCCTCT	
NM_000364	Cardiac troponinT (cTnT)	Sense: GCGCTGATTGAGGCTCACTT	80
		Antisense: CGTCTCTCGATCCTGTCTTTGA	
X65964	Nestin	Sense: CAACAGCGACGGAGGTCTC	163
		Antisense: CCTCTACGCTCTCTTCTTTGAGT	
NM_002374	Microtubule Associated protein (MAP2)	Sense: CAGGAATTGACTCCCTCTACAGC	80
		Antisense: TCTTCACCAGGCTTACTTTGC	
NM_002500	Neurogenic differentiation 1 (NeuroD1)	Sense: GCCTTGCTATTCTAAGACGCA	156
		Antisense: GTGGGTTGGGATAAGCCCTT	
NM_006160	Neurogenic differentiation 2 (NeuroD2)	Sense: CCCGACCACGAGAAAAGCTAC	152
		Antisense: TGGTGAAGGTGCATATCGTAAGA	

substrate three to four times to dissolve the film completely. 2% bovine serum albumin (BSA) was used to passivate the un-patterned region. All the substrates were UV sterilized for 15 min before use. Finally, hMSCs were harvested and seeded at a density of 800 cells cm^{-2}.

Quantitative Real Time Polymerase Chain Reaction (qRT-PCR): The qRT-PCR was performed according to the methods previous described[34] on a CFX96 real time PCR detection system (Bio-Rad Laboratories) with KAPA SYBR FAST master mix universal. Primers specific to the targeted genes were obtained from primer bank[35] and were listed in **Table 1**. Relative quantification of gene expression was analyzed with Relative Expression Software Tool 2009.[36] GAPDH and β-actin were used as endogenous housekeeping genes.

Immunostaining and In Situ Proximity Ligation Assay (PLA): Immunostaining was performed according to the methods described previously.[37] The primary antibodies were anti vinculin (1:400, Millipore), COLI (1:200, Novus), integrin β_3 (ITB3, 1:100, Millipore), myosin light chain kinase (MLCK, 1:100, Sigma), myosin heavy chain (MHC, 1:100, Abcam), RUNX2 (1:100, Santa Cruz Biotechnology), Osteocalsin (Ocal, 1:100, Santa Cruz Biotechnology) and MAP2 (1:10000, Abcam). Secondary antibodies were TRITC-Phalloidin (1:400, Millipore), Alexa Fluor 488 goat anti mouse IgG (1:400, Invitrogen), and Cy3 goat anti rabbit IgG (1:400, Millipore). For PLA, samples were fixed with 4% paraformaldehyde and then blocked for 1 h with 5% normal goat serum (NGS) in PBS containing 0.1% Triton-X, followed by incubation overnight at 4 °C with mouse anti-heavy chain cardiac myosin antibody (MHC) (1:100, Abcam) in NGS. Duolink *in situ* PLA was performed as recommended by the manufacturer (OLink Biosciences). The cells and methods used for positive control of differentiation makers were mentioned in the SI. The negative control was performed without primary antibody. Images were taken using an Eclipse 80*i* microscope (Nikon) using 20× objective lens.

Image Analysis and Statistic Study: Immunostained and PLA images were analyzed with ImageJ 1.44f as previously described.[38] In brief, the image was converted to 8 bit, and threshold was adjusted automatically by "Adjust threshold" function. After that, the size and morphology of FA were analyzed by the "Analyze particles" function. The PLA images were also analyzed using the same "Analyze particles" function as FA, the number of positive red dots of each cells was calculated. 100 cells were analyzed in each group for vinculin statistical study and 26 cells were analyzed in each group for PLA analysis. All assays were triplicated for each time point and were expressed as means ± standard deviation (SD). Statistical analysis was performed by using a one-way ANOVA followed by Tukey's pair wise comparisons. A value of $p < 0.05$ was considered statistically significant.

Supporting Information

Supporting Information is available from the Wiley Online Library or from the author.

Acknowledgements

We would like to acknowledge Singapore Stem Cell Consortium (SSCC) (Grant no: SSCC/09/017) and Nanyang Technological University, Singapore, for financial support.

Received: April 27, 2012
Revised: July 5, 2012
Published online: October 1, 2012

[1] K. Lee, D. Mooney, *Chem. Rev* **2001**, *101*, 1869.
[2] W. J. Rogers, J. G. Canto, C. T. Lambrew, A. J. Tiefenbrunn, B. Kinkaid, D. A. Shoultz, P. D. Frederick, N. Every, *J. Am. Coll.Cardiol.* **2000**, *36*, 2056.
[3] a) D. G. Phinney, D. J. Prockop, *Stem Cells* **2007**, *25*, 2896; b) Y. Jiang, B. Jahagirdar, R. Reinhardt, R. Schwartz, C. Keene, X. Ortiz-Gonzalez, M. Reyes, T. Lenvik, T. Lund, M. Blackstad, *Nature* **2002**, *418*, 41.
[4] J. A. Burdick, G. Vunjak-Novakovic, *Tissue. Eng. Part A* **2009**, *15*, 205.
[5] C. A. Reinhart-King, M. Dembo, D. A. Hammer, *Biophys. J.* **2008**, *95*, 6044.
[6] R. J. Pelham, Y.-l. Wang, *Proc. Natl. Acad. Sci. U. S. A.* **1997**, *94*, 13661.
[7] R. G. Wells, *Hepatology* **2008**, *47*, 1394.
[8] D. E. Discher, D. J. Mooney, P. W. Zandstra, *Science* **2009**, *324*, 1673.
[9] a) A. J. Engler, S. Sen, H. L. Sweeney, D. E. Discher, *Cell* **2006**, *126*, 677; b) C. Y. Tay, M. Pal, H. Yu, W. S. Leong, N. S. Tan, K. W. Ng, S. Venkatraman, F. Boey, D. T. Leong, L. P. Tan, *Small* **2011**, *7*, 1416.
[10] M. A. Wozniak, K. Modzelewska, L. Kwong, P. J. Keely, *Biochim. Biophys. Acta-Mol. Cell Res.* **2004**, *1692*, 103.
[11] C. Y. Tay, H. Yu, M. Pal, W. S. Leong, N. S. Tan, K. W. Ng, D. T. Leong, L. P. Tan, *Exp. Cell Res.* **2010**, *316*, 1159.
[12] a) R. J. McMurray, N. Gadegaard, P. M. Tsimbouri, K. V. Burgess, L. E. McNamara, R. Tare, K. Murawski, E. Kingham, R. O. C. Oreffo, M. J. Dalby, *Nat Mater* **2011**, *10*, 637; b) M. J. Dalby, N. Gadegaard, R. Tare, A. Andar, M. O. Riehle, P. Herzyk, C. D. W. Wilkinson, R. O. C. Oreffo, *Nat Mater* **2007**, *6*, 997.
[13] D. Lehnert, B. Wehrle-Haller, C. David, U. Weiland, C. Ballestrem, B. A. Imhof, M. Bastmeyer, *J Cell Sci* **2004**, *117*, 41.
[14] N. Xia, C. K. Thodeti, T. P. Hunt, Q. Xu, M. Ho, G. M. Whitesides, R. Westervelt, D. E. Ingber, *FASEB J.* **2008**, *22*, 1649.
[15] J. M. Goffin, P. Pittet, G. Csucs, J. W. Lussi, J.-J. Meister, B. Hinz, *J. Cell Biol.* **2006**, *172*, 259.
[16] J. C. Lötters, W. Olthuis, P. H. Veltink, P. Bergveld, *J MicroMech Microeng* **1997**, *7*, 145.
[17] S. Takayama, E. Ostuni, X. Qian, J. C. McDonald, X. Jiang, P. LeDuc, M. H. Wu, D. E. Ingber, G. M. Whitesides, *Adv. Mater.* **2001**, *13*, 570.
[18] a) A. J. Engler, M. A. Griffin, S. Sen, C. G. Bonnetnann, H. L. Sweeney, D. E. Discher, *J. Cell Biol.* **2004**, *166*, 877; b) A. I. Teixeira, S. Ilkhanizadeh, J. A. Wigenius, J. K. Duckworth, O. Inganäs, O. Hermanson, *Biomaterials* **2009**, *30*, 4567.
[19] D. Reynolds, M. Lord, *Med Biol Eng Comput* **1992**, *30*, 419.
[20] a) J. L. Wilbur, A. Kumar, E. Kim, G. M. Whitesides, *Advanced Materials* **1994**, *6*, 600; b) A. Perl, D. N. Reinhoudt, J. Huskens, *Adv. Mater.* **2009**, *21*, 2257.
[21] H. Yu, L. P. Tan, *US Provisional Patent, Appl. No. 61/406*, *385*, **2010**.
[22] H. Yu, S. Xiong, C. Y. Tay, W. S. Leong, L. P. Tan, *Acta Biomate.* **2012**, *8*, 1267.
[23] C. S. Chen, J. L. Alonso, E. Ostuni, G. M. Whitesides, D. E. Ingber, *Biochem. Biophys. Res. Commun.* **2003**, *307*, 355.
[24] P. LeDuc, E. Ostuni, G. Whitesides, D. Ingber, in *Method Cell Biol.*, Vol. *69*, Academic Press, **2002**, 385.
[25] T. Yeung, P. C. Georges, L. A. Flanagan, B. Marg, M. Ortiz, M. Funaki, N. Zahir, W. Y. Ming, V. Weaver, P. A. Janmey, *Cell Motil. Cytoskel.* **2005**, *60*, 24.
[26] V. Dugina, L. Fontao, C. Chaponnier, J. Vasiliev, G. Gabbiani, *J Cell Sci* **2001**, *114*, 3285.
[27] B. Hinz, V. Dugina, C. Ballestrem, B. Wehrle-Haller, C. Chaponnier, *Mol. Biol. Cell* **2003**, *14*, 2508.
[28] L. E. McNamara, R. Burchmore, M. O. Riehle, P. Herzyk, M. J. P. Biggs, C. D. W. Wilkinson, A. S. G. Curtis, M. J. Dalby, *Biomaterials* **2012**, *33*, 2835.
[29] O. M. Rossier, N. Gauthier, N. Biais, W. Vonnegut, M.-A. Fardin, P. Avigan, E. R. Heller, A. Mathur, S. Ghassemi, M. S. Koeckert, J. C. Hone, M. P. Sheetz, *EMBO J* **2010**, *29*, 1055.
[30] R. McBeath, D. M. Pirone, C. M. Nelson, K. Bhadriraju, C. S. Chen, *Dev. Cell* **2004**, *6*, 483.
[31] M. A. Griffin, S. Sen, H. L. Sweeney, D. E. Discher, *J Cell Sci* **2004**, *117*, 5855.
[32] W. S. Leong, C. Y. Tay, H. Yu, A. Li, S. C. Wu, D.-H. Duc, C. T. Lim, L. P. Tan, *Biochem. Bioph. Res. Co.* **2010**, *401*, 287.
[33] H. Li, J. Zhang, X. Zhou, G. Lu, Z. Yin, G. Li, T. Wu, F. Boey, S. S. Venkatraman, H. Zhang, *Langmuir* **2009**, *26*, 5603.
[34] H. Yu, C. Y. Tay, W. S. Leong, S. C. W. Tan, K. Liao, L. P. Tan, *Biochem. Biophys. Res. Co.* **2010**, *393*, 150.
[35] X. Wang, B. Seed, *Nucl. Acids Res.* **2003**, *31*, e154.
[36] M. W. Pfaffl, G. W. Horgan, L. Dempfle, *Nucl. Acids Res.* **2002**, *30*, e36.
[37] C. Y. Tay, H. Gu, W. S. Leong, H. Yu, H. Q. Li, B. C. Heng, H. Tantang, S. C. J. Loo, L. J. Li, L. P. Tan, *Carbon* **2010**, *48*, 1095.
[38] W. Y. Yeong, H. Yu, K. P. Lim, K. L. G. Ng, Y. C. F. Boey, V. S. Subbu, L. P. Tan, *Tissue. Eng. Part C: Methods* **2010**, *16*, 1011.
[39] B.-R. Son, L. A. Marquez-Curtis, M. Kucia, M. Wysoczynski, A. R. Turner, J. Ratajczak, M. Z. Ratajczak, A. Janowska-Wieczorek, *Stem Cells* **2006**, *24*, 1254.